# ENDOR - ODENDOR

J.-M. SPAETH

*University of Paderborn, FB 6, Physik, Warburger Str. 100A, D-4790 Paderborn, F.R.G.*

Résumé - Les developments récents dans la spectroscopie E.N.D.O.R. afin de déterminer les structures des défauts ponctuels dans les semiconducteurs sont resumés brèvement. L'état actuel est illustré pour l'E.N.D.O.R. conventionel et pour l'E.N.D.O.R. détecté par l'optique (O.D.E.N.D.O.R.) avec des résultats récents en partie non publiés comme pour la lacune de gallium dans GaP et pour les défauts 'anti-site' ($As_{Ga}$) dans GaAs.

Abstract - Recent developments in electron nuclear double resonance (ENDOR) spectroscopy to determine defect structures in semiconductors are briefly reviewed. The present state is illustrated for both conventional ENDOR and optically detected ENDOR (ODENDOR) with some recent published and unpublished results for the Ga-vacancy in GaP and the anion antisite defects in ($As_{Ga}$) in GaAs.

## I - INTRODUCTION

In semiconductors physics electron spin resonance (ESR) is a well established method to study point defects. In practice, however, with ESR defect structures can be determined only in some favourable cases, if the hyperfine (hf) structure with the ligands and possibly a central nucleus is resolved. In general, one has to resort to the method of electron nuclear double resonance (ENDOR), which allows the resolution of ligand or superhyperfine (shf) interactions. The method was originally introduced by G. Feher to study shallow donors in Si /1/ and developed further by H. Seidel /2/. Investigations in both semiconductors and ionic crystals soon showed that ENDOR spectra are mostly complicated and not easy to measure nor to analyse. In recent years progress was made by computer-assisted experiments and the application of advanced ENDOR techniques like ENDOR-induced ESR /3/ and DOUBLE ENDOR /4/. This will be illustrated with some examples including yet unpublished results on the Ga-vacancy in GaP.

Optical detection of magnetic resonance is an established highly sensitive technique for semiconductors using the donor-acceptor recombination fluorescence /5/. However, no ENDOR experiments with this technique were reported with resolved ligand hf interactions. Recently, in GaAs, by measuring the optical detection of magnetic resonance via the magnetic circular dichroism of the absorption, a technique developed originally for the study of colour centres in ionic crystals /6/, not only a high sensivity could be achieved for ESR /7/, but also ENDOR could be measured with resolution of the ligand hf interactions of several neighbour shells /8/. The method will be briefly explained and new results on the anion antisite defects in GaAs will be presented. By measuring the photo-excitation spectrum of the optically detected ESR and ENDOR spectra and the photoquenching behaviour it could be shown, that the $As_{Ga}$-$As_i$ complex identified to be the 'antisite' defect in as-grown s.i.

GaAs has the same optical and photoquenching properties as the EL2 defect and can therefore be identified with it /9/.

## II - COMPUTER ASSISTED ELECTRON NUCLEAR DOUBLE RESONANCE (ENDOR)

From the symmetry of the ligand hf interactions one can determine the site of the defect, from the size the electronic structure. For impurity centres the hf interaction with the central nucleus allows its chemical identification. The ligand hf structure can be resolved by ENDOR experiments, in which the nuclear magnetic resonance (NMR) transitions of nuclei coupled to the unpaired electron(s) are detected by measuring the change of the partly saturated ESR transition /2/. A direct detection of the NMR is not possible because the defect concentration is too low. The double resonance experiment gives a sensitivity enhancement of several orders of magnitude compared to NMR and a hf resolution enhancement compared to ESR. The spin Hamiltonian for the paramagnetic defect is

$$H = \mu_B \vec{B}_o \tilde{g} \vec{S} + \sum_{\alpha=1}^{n} (\vec{I}_\alpha \tilde{A}_\alpha \vec{S} + \vec{I}_\alpha \tilde{Q}_\alpha \vec{I}_\alpha - g_{I,\alpha} \mu_n \vec{B}_o \vec{I}_\alpha) \qquad (1)$$

It contains the electron Zeeman, hf, quadrupole and nuclear Zeeman energies. The sum runs over the central nucleus and all interacting ligands /12/. The ENDOR (NMR) frequencies are given in first order perturbation theory by

$$\nu(m_s) = \frac{1}{2} \left| m_s(a+b(3\cos^2\gamma-1) \mp g_I \mu_n B_o \pm 3m_q \cdot q(3\cos^2\gamma'-1) \right| \qquad (2)$$

where the isotropic hf constant a and the anisotropic hf constant b and the quadrupole constant q are related to their respective tensors by

$$A_{zz} = a+2b, \quad A_{xx} = A_{yy} = a-b, \quad Q_{zz} = 2q, \quad Q_{xx} = Q_{yy} = -q \qquad (3)$$

$\gamma$ and $\gamma'$ are the angles between the principal axes with the largest interaction and the magnetic field. $m_q = (m_I + m_I')/2$, the average between the two nuclear spin quantum numbers, which are connected by the NMR transition /11,13/. For simplicity, axially symmetric tensors are assumed. Without quadrupole interaction each ligand nucleus gives rise to $(2m_s+1)$ ENDOR lines. The approximation of equ.(2) holds only for simple cases /11/.

Figs. 1a and 1b show as an example the ENDOR line angular dependence of $Te^+$ donors in Si. The magnetic field was rotated in a (110) plane from [100] through [111] to [110]. The dots are the line peaks, the curves are calculated angular dependencies after determination of the spin Hamiltonian parameters according to equ.(1) to (3) /12/. Altogether 12 different shells of neighbour nuclei could be identified. The $^{29}Si$ shf interaction could be determined with 3 shells of [111] symmetry, 2 shells of [100] symmetry and 7 shells of [110] symmetry. From the ENDOR analysis follows safely, that the effective spin is 1/2 and not 3/2 and thus the charge state of $Te^+$ could be inferred. It could also be safely said, that the $Te^+$ occupies either a substitutional or a $T_d$ interstitial site. However, between the two sites cannot be distinguished, since the neighbour nuclei are of the same symmetry type about the two sites and only this can be analysed in the experiment. For a decision between the sites some knowledge about the wave function (radial behaviour) would be needed to be compared with the shf parameters /12/. Meanwhile, it is established by theory that the substitutional site is energetically favoured /13/.

In many cases there is a big number of ENDOR lines for each crystal orientation. For thermal donors in Si over 100 ENDOR lines were measured in the frequency range between 0.5 and 8 MHz /14/ and for $Ni^{3+}$ in GaP more than 500 ENDOR lines for each crystal orientation. Fig. 2 shows a section of the ENDOR line angular dependence for different $^{69}Ga$ and $^{71}Ga$ neighbours for $Ni^{3+}$ in GaP /15/. The investigations

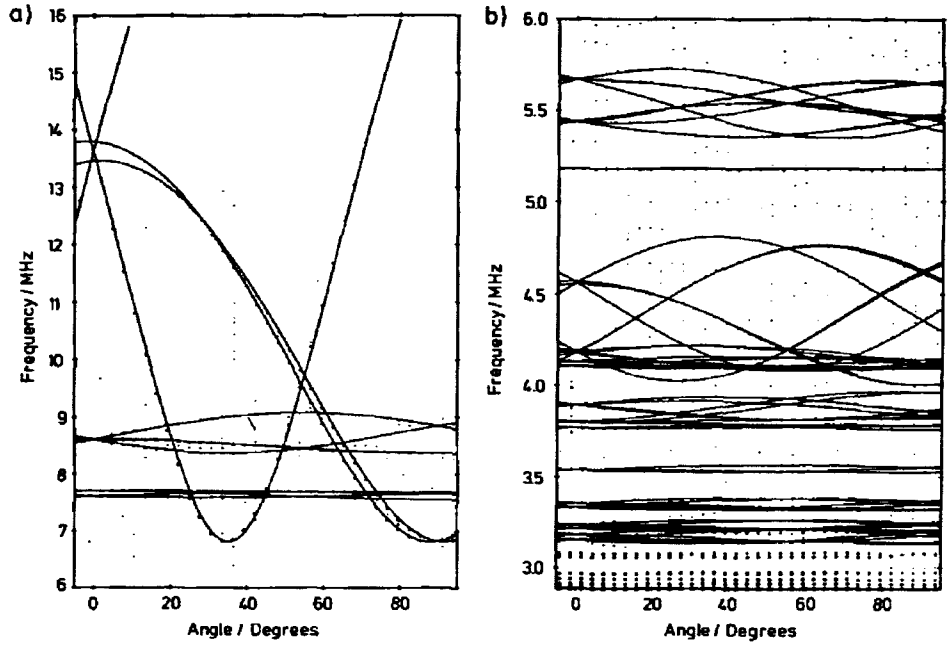


Fig. 1 – ENDOR angular dependence of $Te^+$ defects in Si. The magnetic field was rotated in a (110) plane. $0^o \triangleq [100]$. After /12/.

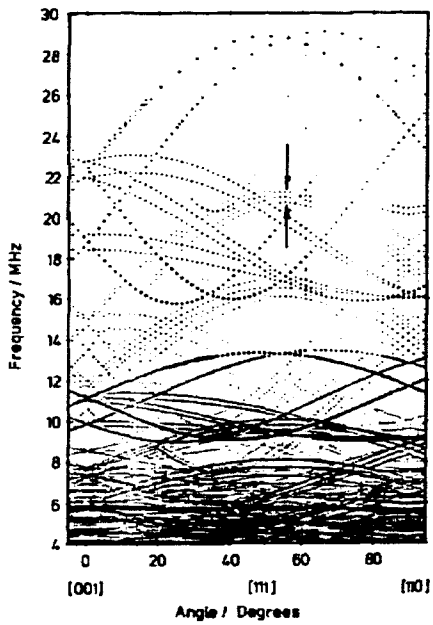


Fig. 2 – Section of the ENDOR angular dependence of $Ni^{3+}$ defects in GaP. The lines are due to $^{31}P$, $^{69}Ga$ and $^{71}Ga$ neighbours. After /15/.

of defects with so many ENDOR lines are only feasible by using computer-assisted ENDOR spectrometers for automated measurements of the angular dependence in small angular steps, in order to be able to follow the angular patterns. Digital filters can be applied to the spectra to improve the signal to noise ratio /16/. The frequency position of the lines are determined by applying special peak-search algorithms and deconvolution procedures /17/. The dots in Figs. 1 and 2 were obtained in such a way. The lines at ∿21 MHz for $B_o \| \sim[111]$ in Fig. 2 are $^{69}Ga$ lines (I = 3/2 h) split by a small quadrupole interaction to triplets. It followed from the ENDOR analysis that S = 3/2, thus it was confirmed that the defect is due to $Ni^{3+}$ /15/. As for the site of $Ni^{3+}$ the same principal difficulty exists as discussed for $Te^+$ in Si: from the ENDOR analysis alone the substitutional site cannot be distinguished from the $T_d$ interstitial site. However, in the case of the $Ni^{3+}$ a theoretical estimate of the experimental Ga-quadrupole interaction constants allowed the assignment to a substitutional site /15/.

With ENDOR also small distortions of a defect can be resolved. Such a distortion causes a lowering of symmetry of the defect such that the near neighbours are not all equivalent as in high symmetry. In the ENDOR spectrum all the orientations of such a defect would occur. In the spectrum near-neighbour lines would appear with additional small 'splittings' of

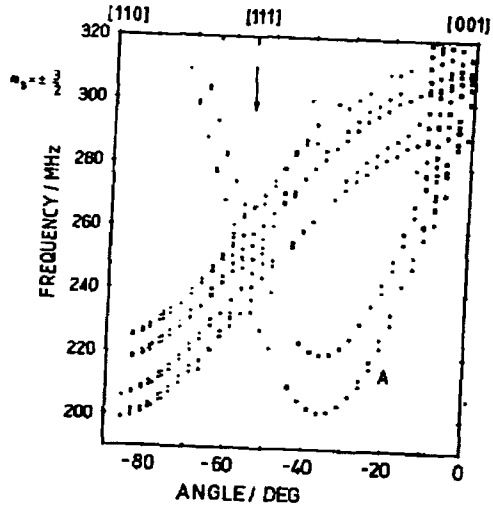


Fig. 3 - Part of the angular dependence of ENDOR lines of nearest P-neighbours of the Ga-vancancy in GaP. The magnetic field was rotated in a (110)-plane. (X-band).

the ENDOR lines. A recent observation of small splittings of a 'normal' ENDOR angular pattern is that shown in Fig. 3, in which a section of the high frequency ENDOR angular dependence of the Ga-vacancy in GaP is reproduced. Its ESR spectrum was first investigated by Kennedy and Wilsey /18/. Already a rough analysis according to equ.(2) confirmed that S = 3/2, as was proposed earlier from ESR experiments under uniaxial stress /19/, and that the ENDOR lines of Fig. 3 are due to nearest P-neighbours (I = 1/2). However, if one assumes a perfect tetrahedral symmetry and solves equ.(1) in perturbation theory to 2nd order including the effect of pseudo-dipolar coupling of the 4 nearest P nuclei via their isotropic hf interaction /20/, one cannot explain the high number of lines in Fig. 3. The small observed splittings are suggestive of a slight distortion of the defect. It was excluded by ENDOR-induced ESR experiments, a kind of ENDOR-line excitation spectroscopy, that different defects are superimposed in the ESR spectrum causing additional ENDOR lines /5/. The experimental proof, that the defect has indeed perfect tetrahedral symmetry, could be given by performing DOUBLE-ENDOR experiments (triple resonance). Two NMR frequencies are applied simultaneously and the influence of one ENDOR transition on the 2nd one is monitored. There is a signal only, if both nuclei belong to the same defect. Otherwise, they are not coupled. A DOUBLE-ENDOR signal is measured only, if both nuclei belong to the same defect orientation in case of low symmetry defects /4/. Fig. 4 shows the DOUBLE-ENDOR spectrum for $B_o$ near [111]. In both spectra all lines appear proving that the vacancy is not a low symmetry defect. The occurence of so many lines proved to be the result of a coupling between the different P-neighbour nuclei, which could be understood quantitatively by diagonalising the spin Hamiltonian numerically. The additional splittings compared to earlier treatments of this effect /20/ are due to the large anisotropic part of the ligand hf interaction. Thus the Ga-vacancy has S = 3/2, perfect tetrahedral symmetry and the interaction parameters a = 195 MHz, b = 54.5 MHz for the nearest P-neighbours. The interaction with one more P and one Ga shell could also be resolved /22/.

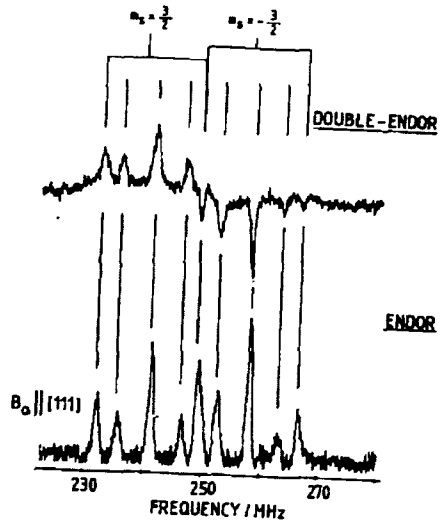


Fig. 4 - ENDOR and DOUBLE ENDOR spectrum of nearest P-neighbour lines of the Ga-vacancy in GaP for $B_o$ approx. parallel to [111].

## III - OPTICAL ABSORPTION DETECTED ESR AND ENDOR

The detection of ESR and ENDOR via the optical absorption is based on its magnetic circular dichroism (MCD). In Fig. 5a a simplified free atom model for an s→p transition in a magnetic field presents the essential features. In a crystal the two circular polarised absorption transitions ($\sigma_+$ and $\sigma_-$), are approximately the derivative of the absorption band, if the spin orbit splitting $\Delta_{s.o.}$

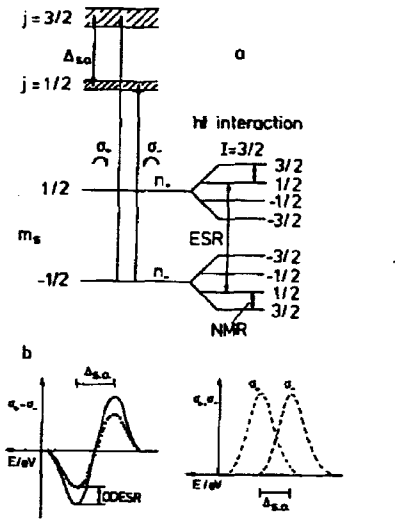


Fig. 5 - Simplified level scheme to explain the magnetic circular dichroism of the absorption and the optical detection of the electron spin resonance and electron nuclear double resonance (not to scale).

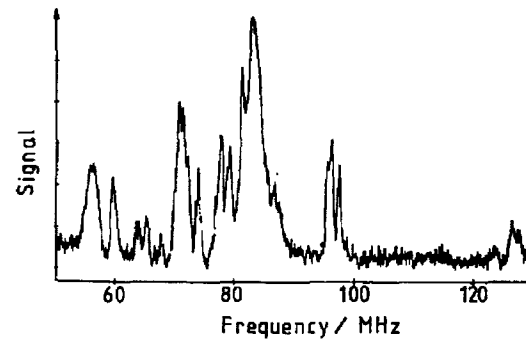


Fig. 6 - Part of the optically detected ENDOR spectrum of anion antisite defects in s.i. as-grown, undoped GaAs for $B_o$ in a (110)-plane. T = 1.5 K, $\nu$ = 24 GHz.

in the excited state is smaller than the band width. Its peak separation is given by $\Delta_{s.o.}$ (see Fig. 5b). The peak heights of the MCD are given by /21/

$$MCD_{extr} \propto \Delta_{s.o.} \frac{n_- - n_+}{n_- + n_+} \propto \Delta_{s.o.} \tanh \frac{g_e \mu_B B_o}{2kT} \qquad (4)$$

A variation of the relative population numbers $n_+$ and $n_-$ of the electronic Zeeman levels changes the MCD. By ESR transitions the difference in $(n_- - n_+)$ is diminished provided the spin lattice relaxation time $T_1$ is long enough to allow a partial saturation of this transition. By monitoring the decrease of $MCD_{extr}$ the ESR transition can be detected.

An unexpected successful application of this technique was obtained in undoped, semiinsulating 'as-grown' GaAs, although in the optical absorption spectrum no absorption can be detected apart from the very weak EL2 band at 1.18 eV. There is a relatively large MCD between 900 and 1500 nm, which has the shape of two superimposed derivative structures /7/. The ODESR spectrum found was the well known 4 line 'finger-print' spectrum of the anion antisite defects $As_{Ga}$, the 4 line hf splitting being due to a central $^{75}As$ nucleus (I = 3/2). The signal to noise ratio was 2 orders of magnitude better than that of conventional ESR. However, both spectra differed in $T_1$ indicating that the $As_{Ga}$ defects measured optically and conventially must differ in structural details /23,24/. No ligand hf structure is resolved in the ESR spectrum. Conventional ENDOR experiments were not possible due to the weak ESR spectrum. With optical detection ENDOR experiments were successful /8/. Through the ligand hf interactions the level scheme is more complicated than that shown in Fig. 5a. Each of the central $^{75}As$ nuclear Zeeman levels is further split. In order to explain the principle of the mechanism to detect ENDOR optically, it is assumed for simplicity that the hf pattern in Fig. 5a is due to one As ligand. Since in an allowed ESR transition no nuclear spins must flip, each transition causes only a partial decrease of the MCD, in the simplified example only 1/4 of the total de-

crease possible. If simultaneously an NMR transition is induced, additional populations of the nuclear Zeeman levels are included in the ESR transition and hence the decrease of the MCD is stronger. Thus, the change of the ODESR detects the NMR transitions /8/. Fig. 6 shows a section of the ENDOR spectrum of antisite defects in an undoped 'as-grown' (pBN-LEC) s.i. GaAs sample (from MRC), as it was recently measured. The signal is the change of the ODESR effect as a function of the NMR frequencies. The signal to noise ratio of the ENDOR effect is of the same order of magnitude as that of the ODESR effect, a definitive advantage over the conventional ENDOR method. Fig. 7 shows the angular dependence between 40 - 100 MHz. There are more lines below and above that range. The recent measurements are greatly improved compared to first results given in ref. /8/ due to better experimental conditions and more experience with this kind of experiment. The width of the ENDOR lines turned out to be smaller here as well as in a V-doped sample compared to the Cr-doped s.i. sample used in ref. /8/. Many more NMR transitions could be detected.

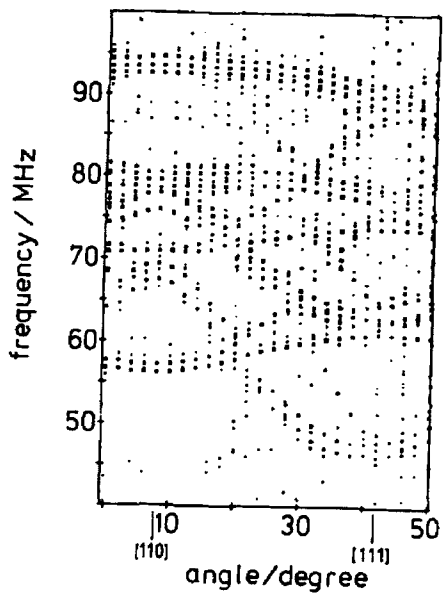


Fig. 7 - Part of the angular dependence of ODENDOR lines of anion antisite defects in s.i. as-grown undoped GaAs for rotation of $B_o$ in a (110)-plane.

The lines of Fig. 7 belong to nearest $^{75}As$ neighbours. A regular antisite defect with 4 tetrahedrally coordinated $^{75}As$ neighbours would have far less ENDOR lines according to equ.(2). However, quite similarly as in the case of the Ga-vacancy in GaP, the 4 nearest neighbours interact via a pseudo-dipolar coupling, which leads to numerous line splittings. There is a large anisotropic hf interaction and a quadrupole interaction. The angular pattern can be understood by numerical diagonalisation of equ.(1). However, there are also ENDOR lines above 100 MHz (see Fig. 6), which can be shown to belong to the same defect. They are also due to $^{75}As$, namely due to one interstitial As atom in the tetrahedral interstitial site. It has [111]-symmetry with respect to the central atom /9/. Fig. 8 shows 2 interstitial sites, the tetrahedral and hexagonal site, pos. 5 and 5', respectively. In table 1 the hf, shf and quadrupole interactions determined from the ODENDOR analysis, are collected. (The interaction constants of ligand 1 and second shell As-neighbours are still approximate values). The $As_{Ga}$ defect has $C_{3v}$ symmetry, the As-neighbours 2, 3 and 4 are equivalent, As-neighbour 1 has a slightly higher isotropic interaction compared to the other three nearest neighbours and the interstitial has a markedly different interaction although it is of the same order /25/. The interstitial ligand must be diamagnetic and is $As_i^-$ or $As_i^+$, otherwise one would have observed a large fine structure splitting in ESR. From the ODENDOR analysis the position of the interstitial relative to the As atom on the Ga site cannot be decided. Since its quadrupole interaction is less than half of that of the ligands 2, 3, 4, it is not likely to be on the $T_d$ interstitial site, since then its distance to the 'central' As would be the same as for the ligands 2, 3, and 4. It is therefore on site 5' or even further away. For a detailed discussion see /25/.

No Ga-ENDOR lines could be detected. If one approximates the wave function for the $As_{Ga}$ defect by the LCAO ansatz

$$|\psi> = \sum_i \eta_i |\psi> \qquad (5)$$

Table 1. Hf, shf and quadrupole constants (MHz) and LCAO spin density of As-ligands of $As_{Ga}$ defects in s.i. GaAs

| As nucleus | $a/h$ | $b/h$ | $q/h$ | $\eta_i^2$(%) |
|---|---|---|---|---|
| central | 2580 | -- | -- | 16 |
| 2,3,4 | 167.8 ±0.2 | 53.9 ±0.2 | 11.7 ±0.2 | 15.8 |
| 1 | ∿ 170 | ∿ 54 | ∿ 12 | 15.7 |
| interstitial | 215 ±2 | 44 ±1 | 4.8 ±0.1 | 13.4 |
| 3rd shell As | ∿ 18 | ∿ 2 | -- | 0.66 |

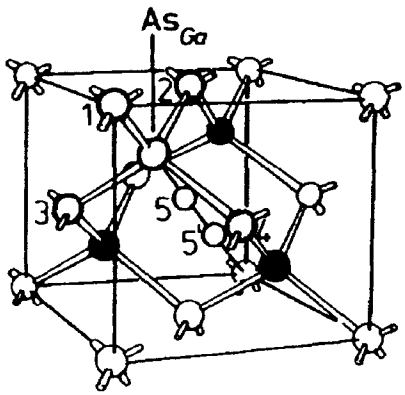


Fig. 8 - Model of the $AsAs_4$-$As_i$ complex.

then $\eta_i^2$ represents that part of $|\psi>$, which is localised at the neighbour i. At each As-site $\psi_i$ are the $sp^3$ hybrids

$$\eta_i^2 = \frac{a_i}{a_f} + \frac{b_i}{b_f} \qquad (6)$$

where $a_f$ and $b_f$ are the isotropic and anisotropic shf constants of the free As-atoms. In table 1 $\eta_i^2$ are given per ligand. They were determined such, that

$$\sum_{i=1}^{18} \eta_i^2 (As_i) = 1 \qquad (7)$$

Approximately the same amount of spin density is localised at each of the 6 As constituants of the $As_4$-$As_i$ complex. Thus, the interstitial is an integral part of the defect (for detailed discussion, ref. /25/.

## IV - CORRELATION OF ESR/ENDOR WITH OPTICAL BANDS AND ENERGY LEVEL POSITIONS

When $B_o$ is set to one particular ODESR line or the NMR frequency to one particular ODENDOR line and these ESR/ENDOR lines are then monitored as a function of the optical wavelength, one measures that part of the MCD, which belongs to this particular paramagnetic defect ("MCD-tagged by ESR or ENDOR") /26/. For the antisite spectra in 'as-grown' material it was found that the total MCD measured belongs to it /7,8/.

A correlation with the energy level positions can be made by photo-ODESR/ODENDOR. In p-type GaAs:Zn (HB, MCP Ltd., $p \sim 4 \cdot 10^{16} cm^{-3}$) the paramagnetic antisite $D^+/D^{++}$ level is empty, since the Fermi level is close to the Zn acceptors. No $As_{Ga}$-MCD can be observed. Upon additional light excitation the level could be populated from the valence band for light with energy $h\nu > 0.52$ eV. For light energies above 0.73 eV the intensity decreased again, upon which an absorption band peaking at 1.2 eV appeared, which is identical with the band ascribed to the EL2 defects. A photo-ODENDOR experiment showed, that the ODESR spectrum is due to the $AsAs_4$-$As_i$ complex. These experiments show that the energy levels of the $AsAs_4$-$As_i$ complex are $E_V$ + 0.52 eV ($D^+/D^{++}$) and $E_V$ + 0.73 eV ($D^o/D^+$). The appearance of the 1.2 eV absorption band and the EL2 like photoquenching behaviour led to the conclusion that the diamagnetic, isolated $As_{Ga}$-$A_i$ complex can be associated with one of the EL2 defects /25/.

References

/ 1/ G. Feher, Phys. Rev. 114, 1219 and 1245 (1959)
/ 2/ H. Seidel, Z. Physik 165, 218 (1961)
/ 3/ J.R. Niklas and J.-M. Spaeth, phys. stat. sol. (b) 101, 221 (1980)
/ 4/ J.R. Niklas, R.U. Bauer and J.-M. Spaeth, phys. stat. sol. (b) 119, 171 (1983)
/ 5/ B.C. Cavenett, Ad. Phys. 30, 475 (1981)
/ 6/ L.F. Mollenauer, S. Pan and S. Yngverson, Phys. Rev. Letts. 23, 689 (1969)
/ 7/ B.K. Meyer, J.-M. Spaeth and M. Scheffler, Phys. Rev. Letts. 52, 851 (1984)
/ 8/ D.M. Hofmann, B.K. Meyer, F. Lohse and J.-M. Spaeth, Phys. Rev. Letts. 53, 1187 (1984)
/ 9/ J.-M. Spaeth, Proc. of the 4th International Conf. on Semi-Insulating III-V Materials, Hakone, Japan, 1986
/10/ G.E. Pake and T.C. Estle, The physical principals of electron paramagnetic resonance, Benjamin Inc., Reading, Mass. (1973)
/11/ H. Seidel, Habilitationsschrift, Stuttgart, 1966
/12/ J.R. Niklas and J.-M. Spaeth, Solid State Comm. 46, 121 (1985)
/13/ F. Beeler, M. Scheffler, O. Jepsen and O. Gunnarson, Phys. Rev.Letts. 54, 2525 (1985)
/14/ J. Michel, J.R. Niklas and J.-M. Spaeth, Proc. of the MSR Fall Meeting, Boston, 1985
/15/ Y. Ueda, J.R. Niklas, J.-M. Spaeth, U. Kaufmann and J. Schneider, Solid State Comm. 46, 127 (1983)
/16/ M.U.A. Bromba and H. Ziegler, Anal. Chem. 56, 2012 (1984)
/17/ J.R. Niklas, Habilitationsschrift, Paderborn, 1983
/18/ T.A. Kennedy and N.D. Wilsey, Phys. Rev. Letts. 41, 977 (1978)
/19/ T.A. Kennedy, N.D. Wilsey, J.J. Krebs and G.H. Stauss, Phys. Rev. Letts. 50, 1281 (1983)
/20/ T.E. Feuchtwang, Phys. Rev. 126, 1628 (1962)
/21/ C.H. Henry and C.P. Slichter in: Physics of Color Centers, Chapter 6, Ed. by W.B. Fowler, Acad. Press, N.Y. (1968)
/22/ J. Hage, J.R. Niklas and J.-M. Spaeth, to be published
/23/ B.K. Meyer and J.-M. Spaeth, J. Phys. C: Solid State Phys. 18, L99 (1985)
/24/ J.-M. Spaeth, D.M. Hofmann and B.K. Meyer, MRS Symposia Proceed. 46, 185 (1985)
/25/ B.K. Meyer, D.M. Hofmann and J.-M. Spaeth, to be published
/26/ F.J. Ahlers, F. Lohse, J.-M. Spaeth and L.F. Mollenauer, Phys. Rev. B28, 1249 (1983)